CHEMICAL ENGINEERING TRANSACTIONS
VOL. 61, 2017
A publication of AIDIC
The Italian Association of Chemical Engineering
Online at www.aidic.it/cet
Guest Editors: Petar S Varbanov, Rongxin Su, Hon Loong Lam, Xia Liu, Jiří J Klemeš

ISBN 978-88-95608-51-8; **ISSN** 2283-9216
DOI: 10.3303/CET1761322

Effect of Throat Length on Steam Ejector Critical Back Pressure

Rongshan Bi*, Mingming Hu, Sigui Wang, Xinshun Tan, Shiqing Zheng

Research Center for Computer and Chemical Engineering, Qingdao University of Science & Technology, Qingdao, 266042, Shan-Dong Province, China
birongshan@163.com

Steam ejector is widely applied in chemical industry and many papers have published to investigate the structure configuration effects on the performance. Previous studies showed that the throat length of steam ejector has little influence on its performance. In this study, Computational Fluid Dynamics model of steam ejector is established to investigate the effects of ejector's throat on its performance. The result shows that ejector's length has little influence on its entrainment ratio. But, there is optimum throat length corresponding to biggest critical back pressure and which is corresponding with the biggest operating flexibility of steam ejectors. So, ejector's throat length has an important effect on its operating flexibility and cannot be over-looked during the design process of steam ejectors.

1. Introduction

The steam ejector is a kind of fluid equipment wildly used in industry filed. It uses high speed primary fluid to produce the low-pressure environment and this environment could volume the secondary fluid (Valle et al., 2015). Ejector is widely used in energy recovery (Ariafar et al., 2016), desalination systems and other industries. Many researchers have studied the principal mechanism inside the steam ejectors, and proposed mathematical models for equipment computation and design. Keenan and Neumann (Keenan et al., 1950) firstly presented the equal-area mixture theory based on one-dimensional gas dynamic theory. Equal-area theory provided theoretical basis for early design of ejector. Ferraro et al (Ferraro et al., 2014) developed isotonic mixture theory, who considered that mixture process between these two kinds of fluid operated under constant-pressure environment. This mixture theory has been adopted in this study. With development of computer technology and fluid dynamics, some researchers attempted to apply Computational Fluid Dynamics (CFD) in modeling the flow field of steam ejector (Wu et al., 2014). Ruangtrakoon et al (2013) tried to find out the effect of nozzle's structure on ejector's performance by commercial CFD package. He concluded that shocks had important influence on ejector's performance. Shocks' performance has been chosen to be the key research point in this study on the basis of Ruangtrakoon's research. Shah et al simulated the flow of saturated vapor, and found the optimum mixing chamber convergent angle θ by numerical simulations (Shah et al., 2014). The result showed that, the difference of ejector's performance under several θ was very large. But they ignored the effect of ejector's throat length for ejector's performance. In this work, effects of ejector throat length on ejector's internal flow characteristics and performance are investigated, and results showed that the throat length has important effect on the ejector's critical back pressure. These results clarified the previous misunderstandings of the throat length and confirmed that the throat length has important effect on the operating flexibility of steam ejectors.

2. CFD model and validation

2.1 Geometrical model

A schematic view of a typical supersonic steam ejector is shown in Figure 1. As high-pressure steam, known as "primary fluid", introduced to the primary nozzle, it fans out with supersonic speed and very low-pressure region at the primary nozzle outlet and in the mixing chamber. Secondary fluid is drawn into the mixing chamber and accelerated by the pressure difference between the secondary fluid and the primary nozzle outlet. By the end of the mixing chamber, the two streams are completely mixed and the speed and static pressure are resumed constant. This mixed stream is further compressed as it flows through the diffuser. Main geometrical parameters of the steam ejector used in this paper are listed in Table 1(Xu et al., 2005).

Please cite this article as: Bi R., Hu M., Wang S., Tan X., Zheng S., 2017, Effect of throat length on steam ejector critical back pressure, Chemical Engineering Transactions, 61, 1945-1950 DOI:10.3303/CET1761322

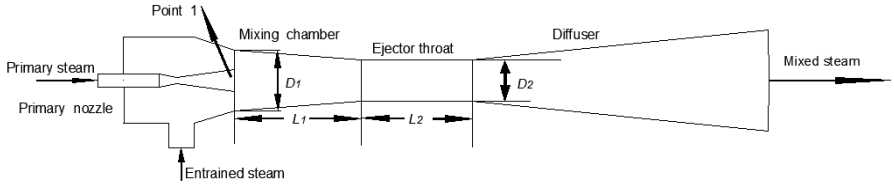

Figure 1: The diagram of the steam-ejector

Table 1: Dimensions of the experimental ejector

Dimension	Value
Nozzle throat diameter (mm)	19.00
Nozzle inlet diameter (mm)	57.00
Nozzle outlet diameter (mm)	76.00
Nozzle divergence angle (°)	20.00
Mixing chamber inlet diameter D1(mm)	187.00
Mixing chamber length L1 (mm)	754.00
Ejector throat diameter D2 (mm)	136.00
Ejector throat length L2 (mm)	374.00
Diffuser outlet diameter (mm)	236.00
Diffuser length (mm)	855.00

2.2 Mathematical model

For the problem of compressible fluid flow, Navier-Stokes (N-S) equations can explain actual situation accurate (Li et al., 2006), so that the N-S equations are applied in this study. Near wall condition was treated using the “standard wall function” (Sriveerakul et al., 2007), and revised wall function. In order to simulate the fluid flow condition in the ejector, a two equations turbulence model was applied to the whole flow domain based on the realizable k-ε turbulence model. Realizable k-ε turbulence model (Wu et al., 2014) was reported to simulate accurately not only the plane jet and the round jet but also the swirl flow and the separation flow. Boundary conditions of both the primary fluid inlet and secondary fluid inlet of the steam ejector were set as “pressure-inlet”. Mixing fluid outlet of ejector was set as “pressure-outlet”. Saturated water vapor, applied as the working fluid, was assumed to an idea gas (Cardemil et al, 2012). In conclusion, equations of numerical model involved in this study are as follows:

Continuity equation:

$$\frac{\partial \rho}{\partial t} + \frac{\partial (\rho u_i)}{\partial x_i} = 0 \tag{1}$$

Momentum equation:

$$\frac{\partial (\rho u_i)}{\partial t} + \frac{\partial (\rho u_i u_j)}{\partial x_j} = -\frac{\partial p}{\partial x_i} + \frac{\partial \tau_{ij}}{\partial x_j} \tag{2}$$

Energy equation:

$$\frac{\partial (\rho E)}{\partial t} + \frac{\partial [u_i (\rho E + p)]}{\partial x_i} = \nabla \cdot (\alpha_{eff} \frac{\partial T}{\partial x_i}) + \nabla \cdot [u_j (\tau_{ij})] \tag{3}$$

$$\tau_{ij} = \mu_{eff} (\frac{\partial u_i}{\partial x_j} + \frac{\partial u_j}{\partial x_i}) - \frac{2}{3} \mu_{eff} \frac{\partial u_k}{\partial x_k} \delta_{ij} \tag{4}$$

Realizable k-ε turbulence equation:

$$\frac{\partial (\rho k)}{\partial t} + \frac{\partial (\rho k u_i)}{\partial x_i} = \frac{\partial}{\partial x_i} [(\mu + \frac{\mu_t}{\delta_k}) \frac{\partial k}{\partial x_j}] + G_k - \rho \varepsilon - Y_M \tag{5}$$

$$\frac{\partial (\rho \varepsilon)}{\partial t} + \frac{\partial (\rho \varepsilon u_i)}{\partial x_i} = \frac{\partial}{\partial x_i} [(\mu + \frac{\mu_t}{\sigma_\varepsilon}) \frac{\partial \varepsilon}{\partial x_j}] + \rho C_1 S_\varepsilon - \rho C_2 \frac{\varepsilon^2}{k + \sqrt{v\varepsilon}} + C_{1\varepsilon} \frac{\varepsilon}{k} C_{3\varepsilon} C_b \tag{6}$$

$$C_1 = \max[0.43, \frac{\mu}{\eta + 5}], \eta = \frac{Sk}{\varepsilon} \tag{7}$$

3. Validation of the mathematical and numerical model

The two-dimensional axisymmetric model was built to get more reasonable result. Quadrilateral structured grids were divided by Gambit (Wang et al., 2010). Grid independence was tested to guarantee the accuracy and stability of the calculation. Fluent 6.3 was used as the CFD solver. Convergence criterion for the residual error is less than 10^{-6} (Ariafar et al., 2016). Table 2 lists the static pressure and velocity at Point 1 under different grid density. Through the comparison of results in Table 2, the final choice about grid density is cell number of 82,309.

Table 2: Grid independence test and verification results

Cell number	Pressure (Pa)	Errors (%)	Velocity (m/s)	Errors (%)
19080	6406.52	0.490	1126.90	0.09
32897	6403.82	0.449	1127.85	0.08
82309	6396.50	0.334	1127.90	0.04
109289	6383.21	0.126	1127.92	0.03
201008	6375.20	0.011	1127.95	0.01

Simulating the examples in literature to verify the reliability of numerical model, and its operating conditions are as follow: the primary fluid inlet pressure PP is 1,101.325 kPa, the secondary fluid inlet pressure PH is 8.932 kPa, the mixing fluid outlet pressure PC is 31.000 kPa. Figure 2 shows the comparison between simulated data and original data about the axle wire pressure. The result can satisfy the accuracy of the model.

4. Result and discussion

4.1 The effect of ejector throat length to entrainment ratio

From the simulation, we can see that with the increase of ejector throat length L2, there is little change of entrainment ratio. That means ejector throat length has little influence on the entrainment ratio under special operating conditions. To better interpret the conclusion, the internal flow field of the steam ejector is shown in Figure 3. According to previous research, the ejector coefficient had an optimal value when diamond shock wave extended near by the outlet of mixing section. Figure 3 shows that, diamond shock wave length and position basically remain nearly unchanged, so the ejector coefficient keeps unchanged accordingly.

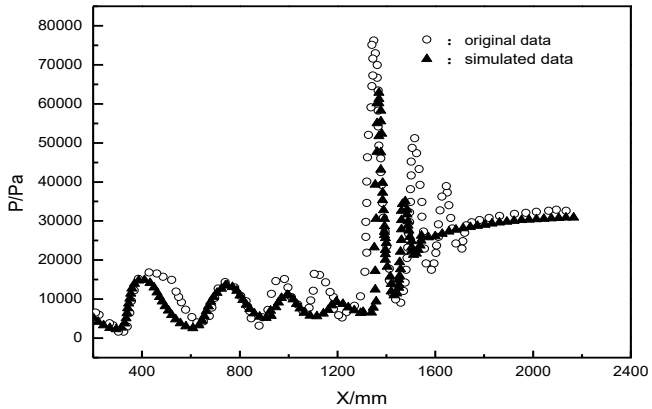

Figure 2: The comparison between simulated data and original data about the axle wire pressure

4.2 The effect of ejector throat length to the critical back pressure

Ejector throat length has little influence on the entrainment ratio. But the normal shock wave and internal friction resistance will increase along the increase of ejector throat length as shown in Figure 3. This can increase the pressure of mixing fluid. The critical back pressure PC, max under different throat length throat was investigated. The critical back pressure PC, max is the biggest mixing fluid outlet pressure for the best performance of steam ejector. Figure 4 shows that, when ejector throat length L2 < 550 mm, the ejector critical back pressure PC, max increases rapidly as the growth of L2. When L2 > 550 mm, PC, max decreases gradually along the growth of L2. For a particular design conditions, therefore, there always be optimal value of L2 corresponds to the maximum critical back pressure PC, max. PC, max means the maximum compression ratio. To ensure larger performance of steam ejector under the requirement of design, L2 should be chosen nearby the optimal value.

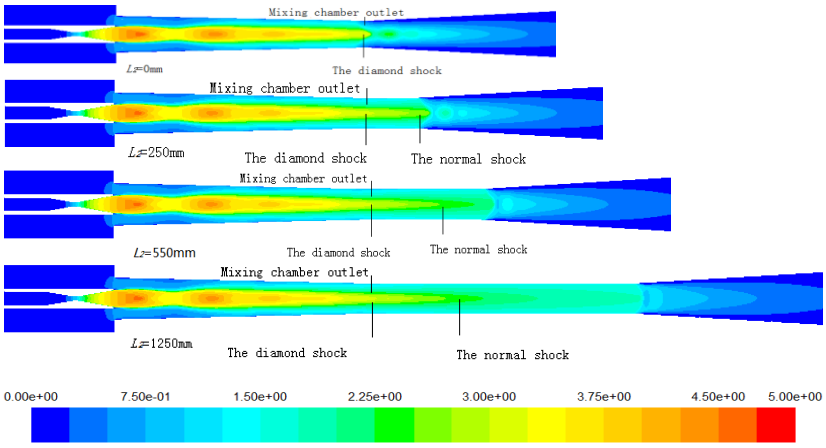

Figure 3: Contours of Mach number under different ejector's throat length

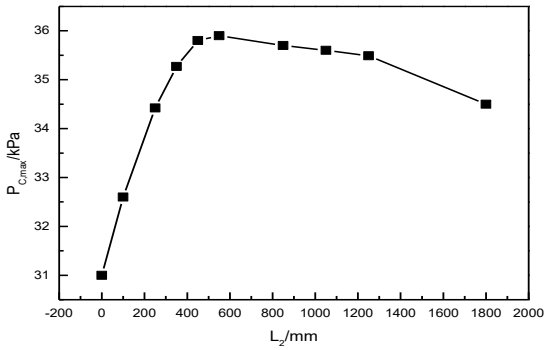

Figure 4: The critical back pressure under different length of ejector's throat

4.3 The effect of ejector throat length to the operating flexibility

For the optimization of steam ejector, greater operating flexibility should be made on the premise of a particular entrainment ratio. This kind of optimization can make rare variation about operating performance with the change of working condition within a certain range. For better interpretation about the effect of ejector throat length to the operating flexibility, a comparison between two structures: ejector1 (L_2 = 250mm), ejector2 (L_2 = 550mm) has been made. The entrainment ratio under different P_C has been shown in Figure 5.

Figure 5 shows that, ejector1, entrainment ratio remained basically unchanged when P_C < 34.00 kPa. Entrainment ratio decreased sharply until negative value when P_C>34.00kPa. Figure 6 shows the fluid flow inside the ejector in this condition. Fluid flows back near the mixing section entrance, and primary fluid flows to incoming road of secondary. This makes the sharp decrease of entrainment ratio. And ejector2 has the same variation tendency to ejector1.

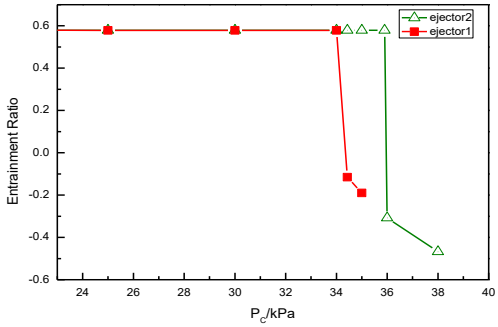

Figure 5: The entrainment ratio under different back pressure

For a special design condition, there is maximum PC which is defined critical back pressure PC, max to keep the optimal value of entrainment ratio. So, keeping PC<PC, max to ensure the steam ejector to work with maximum productivity.

As the length of L2 grows from 250 mm to 550 mm, the PC, max increases by 34.30 kPa to 35.97 kPa. The result means that, in a certain range, PC, max operation flexibility increases with the growth of L2.

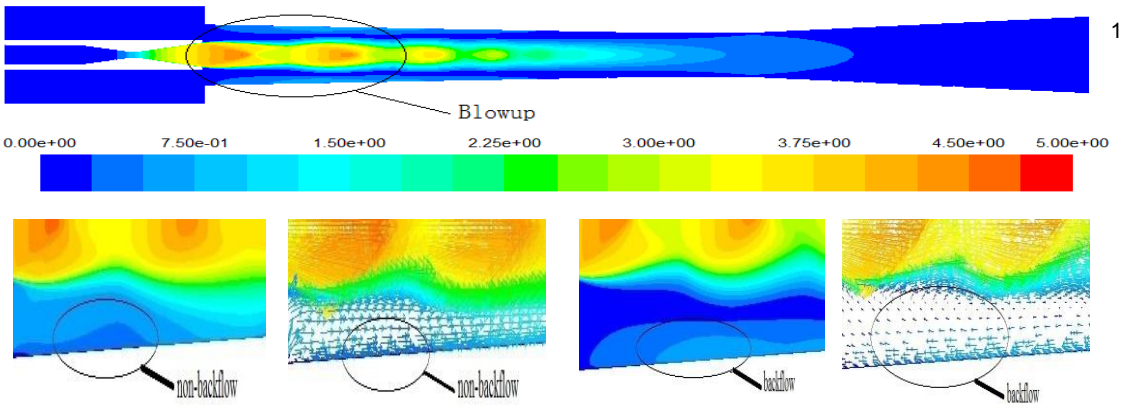

a) P_C = 30.00kPa, non-backflow b) P_C = 35.00kPa, backflow

Figure 6: a) Counters and vectors of back flow under 30.00 kPa; b), Counters and vectors of back flow under 35.00 kPa

Figure 7 shows the effect of secondary fluid inlet pressure PH on the entrainment ratio. From the result， it can be concluded that the entrainment ratio increases with the growth of PH. These changes of entrainment ratio under different PH in both ejector1 and ejector 2 are almost same. The ejector throat length has no effect on the operating flexibility of secondary fluid.

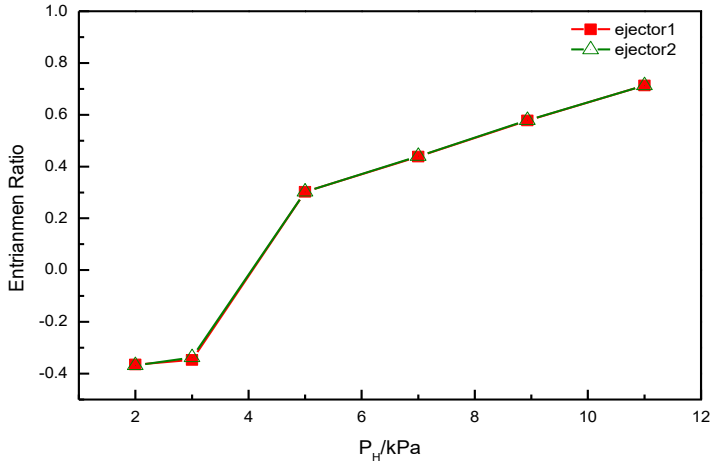

Figure 7: The entrainment ratio under different secondary fluid inlet pressure

5. Conclusion

In this study, 2-dimensional CFD model of steam ejector was built to investigate the effects of ejector throat length on its performance and operating flexibility. The results show that the structure of throat length has important effect on its operating flexibility. For a particular design condition, there is a maximum mixing fluid outlet pressure named critical back pressure under certain entrainment ratio. When mixing fluid outlet pressure lager than its maximum value, ejector's performance rapidly worsened. At a certain operating condition, ejector throat length has little influence on entrainment ratio, but there is optimum throat length corresponding to the maximum operating flexibility. This study can provide basis for optimization of steam ejector.

References

Ariafar K., Buttsworth D., Al-Doori G., Sharifi N., 2016, Mixing layer effects on the entrainment ratio in steam ejectors through ideal gas computational simulations, Energy, 95, 380-392.

Cardemil J.M., Colle S., 2012, A general model for evaluation of vapor ejectors performance for application in refrigeration, Energy Conversion and Management, 64, 79-86.

Ferraro V., Jorge R.F., Cruz I.B., Antunes F., Sarmento B., Castro P.M.L., and Pintado M.E., 2014, In vitro, intestinal absorption of amino acid mixtures extracted from codfish (Gadus morhua, L.) salting wastewater, International Journal of Food Science & Technology, 49(1), 27–33.

Keenan J. H., Neumann E.P., 1950, An investigation of ejector design by analysis and experiment, ASME Journal of Applied Mechanics, 72, 75-81.

Li H.J., Shen S.Q., 2006, Study on special phenomena in the ejector used in a steam ejector refrigerator system, Journal of Engineering Thermophysics, 3, 454-456.

Ruangtrakoon N., Thongtip T., Aphornratana S., Sriveerakul T., 2013, CFD simulation on the effect of primary nozzle geometries for a steam ejector in refrigeration cycle, International Journal of Thermal Sciences, 63, 133-145.

Shah A., Chughtai I.R., Inayat M.H., 2014, Experimental and numerical investigation of the effect of mixing section length on direct-contact condensation in steam jet pump, International Journal of Heat and Mass Transfer, 72, 430-439.

Sriveerakul T., Aphornratana S., Chunnanond K., 2007, Performance prediction of steam ejector using computational fluid dynamics: Part 1. Validation of the CFD results, International Journal of Thermal Sciences, 46(8), 812-822.

Valle G.D.J., Sierra-Pallares J., Carrascal P.G., Ruiz F.C., 2015, An experimental and computational study of the flow pattern in a refrigerant ejector, Validation of turbulence models and real-gas effect, Applied Thermal Engineering, 89, 795-811.

Wang X., Dong J., 2010, Numerical study on the performances of steam-jet vacuum pump at different operating conditions, Vacuum, 84, 1341-134.

Wu H., Liu Z., Han B., Li Y., 2014, Numerical investigation of the influences of mixing chamber geometries on steam ejector performance, Desalination, 353, 15-20.

Xu H.T., Sang Z.F., Gu B., Xu W.D., 2005, Numerical Simulation of the Performance of Steam-Jet Vacuum Pump, Journal of Chemical Engineering of Chinese Universities, 19(1), 22-29.